

# A Study on Kinetics and Mechanism of Thermal Dehydration of Irinotecan Hydrochloride Trihydrate

Praveen C\*, Arthanareeswari M, Kamaraj P, Ravikiran A

Department of Chemistry, SRM University, SRM Nagar, Kattankulathur, Tamilnadu, PIN 603203, INDIA

**Abstract-** The dehydration kinetics of Irinotecan hydrochloride trihydrate (IHT) is analyzed using Thermogravimetric Analysis (TGA) at four different heating rates. The activation energy values were calculated by Ozawa and KAS methods. The calculated activation energy values from both methods are very close to each other. Four calculation procedures based on a single TGA curve and the isoconversional method, as well as 13 mechanism functions were carried out. The mechanism function of dehydration with the integral form  $g(\alpha) = 1 - (1 - \alpha)^{1/3}$  and the differential form  $f(\alpha) = 3(1 - R)^{2/3}$  can be suggested to be the mechanism of phase boundary reaction (spherical symmetry) for the title compound. In this work, the kinetic parameters for the dehydration process of IHT are reported for the first time. Moreover, the Powder X-Ray Diffraction (PXRD) and by Differential scanning calorimetry (DSC) were used to characterize the IHT and the resulted anhydrate form.

**Key words:** Dehydration kinetics; Thermogravimetric analyser; Irinotecan hydrochloride trihydrate; Ozawa method; KAS method.

## I. INTRODUCTION

Active pharmaceutical ingredients (APIs) are known to exist in different solid forms, namely polymorphs, hydrate/solvates and amorphous forms. About one third of APIs are able to form hydrates, the molecular adducts of API with water [1]. During pharmaceutical processing and storage, the stability of hydrates is a concern to pharmaceutical scientists since they may convert to an amorphous form upon dehydration, while others may become chemically labile. For example, cephadrine dihydrate dehydrates and produces an amorphous form that is more easily oxidized [2]. Other hydrates may change their hydration state producing forms with different solubility characteristics, which might impact dissolution rate, stability, drug assay and bioavailability [3]. It is becoming increasingly clear that the solid-state properties (polymorphic form, state of solvation, degree of crystallinity) of the active ingredient can profoundly influence the in vivo performance of the dosage form [4]. Therefore, through understanding of the solid-state stability of solvated drug solids and the kinetics of such transformations, leaves an opportunity to prevent and to have control over the consequent physical changes, which may occur during manufacturing process and shelf life of drug product [5].

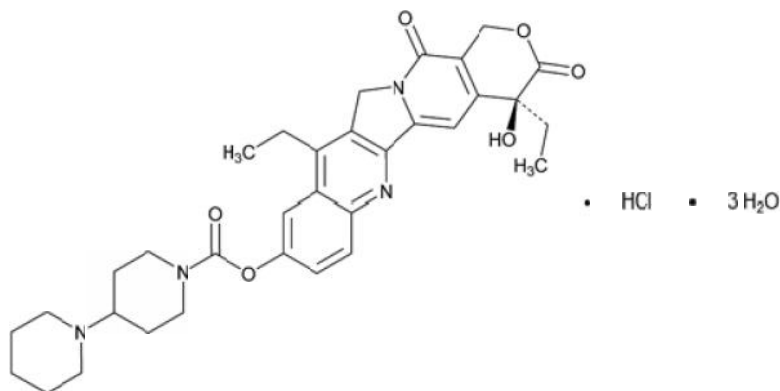


Figure 1: Chemical structure of IHT.

Irinotecan hydrochloride trihydrate (IHT), 7-ethyl-10-[4-(1-piperidino)-1-piperidino] carbonyloxy-camptothecin (Fig.1) is a camptothecin derivative that is highly active against lung and colorectal cancer and has been used for treating several types of tumors. It is sold in the form of the hydrochloride trihydrate salt (CPT-11) under the trade name CAMPTOSAR [6]. In this paper, we have attempted to determine the mechanism model and kinetic (A, E) parameters of the non-isothermal dehydration of the IHT using Thermogravimetric Analysis (TGA) since non-isothermal methods are becoming more widely used because they are more convenient than the classical isothermal methods. The non-isothermal method is based on multiple heating rate data by setting the assumption that the parameters of the model are identical for all heating rates measurements [7]. Various equations of kinetic analyses are known such as the Kissinger [8] (differential method), Ozawa [9], Kissinger-

Akahira-Sunose (KAS) [10] Coats-Redfern, [11] and Van Krevelen et al. [12] methods (integral methods). Especially, the Ozawa and KAS equations were well described and widely used in the literature; therefore, these methods are selected for studying the kinetics of thermal decomposition of the title compound. Moreover, the Powder X-Ray Diffraction (PXRD) and by Differential scanning calorimetry (DSC) were used to characterize the IHT and the resulted anhydrate form.

## II. THEORETICAL CONSIDERATIONS

All kinetics studies are assumed to be based on the following equations:

$$\frac{d\alpha}{dt} = kf(\alpha) \quad (1)$$

And

$$k = Ae^{-\frac{E_a}{RT}} \quad (2)$$

where  $\alpha$  is the extent of conversion and is equal to  $(W_0 - W_t)/(W_0 - W_f)$ ;  $W_0$ ,  $W_t$ , and  $W_f$  are the initial mass of sample, current mass of sample at temperature  $t$ , and final mass at a temperature at which the mass loss is approximately unchanged, respectively.  $f(\alpha)$  is a function depending on the particular decomposition mechanism and is referred to as the differential form. The pre-exponential factor  $A$  ( $\text{min}^{-1}$ ) is assumed to be independent of temperature,  $E$  is the activation energy ( $\text{kJ mol}^{-1}$ ),  $R$  is the gas constant ( $8.314 \text{ J mol}^{-1} \text{ K}^{-1}$ ), and  $k$  is the rate constant. Combination of Equations 1 and 2 gives

$$\frac{d\alpha}{dt} = Af(\alpha)e^{-\frac{E_a}{RT}} \quad (3)$$

Equation 3 can be modified, when  $\beta$  is the heating rate ( $\beta = dT/dt$ ),  $T$  is temperature (K), and  $t$  is time), and the following equation is obtained:

$$\frac{d\alpha}{dt} = \frac{dT}{dt} \frac{d\alpha}{dT} = \beta \frac{d\alpha}{dT} = Af(\alpha)e^{-\frac{E_a}{RT}} \quad (4)$$

Equation 4 can be rearranged to Equation 5 as follows:

$$\frac{d\alpha}{f(\alpha)} = \frac{A}{\beta} e^{-\frac{E_a}{RT}} dT \quad (5)$$

The solution of the left-hand side integral depends on the explicit expression of the function  $f(\alpha)$  and is denoted as  $g(\alpha)$ . Various scientists suggested different ways to solve the right-hand side of Equation 5. Thus, the kinetics of solid state reactions can be described by various equations taking into account the special features of their mechanisms. In kinetic study of IHT, Ozawa and KAS equations were used to determine the activation energy ( $E$ ) and pre-exponential factor ( $A$ ) of the dehydration reaction. These methods are well described and widely used in the literature, which provides reliable results. Therefore, these methods are selected for the kinetic analysis of the dehydration. The equations used for  $E$  calculation are Ozawa equation

$$\ln \beta = \ln \left( \frac{0.0048AE}{g(\alpha)R} \right) - 1.0516 \left( \frac{E}{RT} \right) \quad (6)$$

KAS equation

$$\ln \frac{\beta}{T^2} = \ln \left( \frac{AR}{g(\alpha)E} \right) - \frac{E}{RT} \quad (7)$$

All other parameters are the same as given in Equations 1 and 2. The Arrhenius parameters, together with the reaction model, are sometimes called the kinetic triplet.  $g(\alpha) = \int_0^\alpha d\alpha/f(\alpha)$  is the integral form of  $f(\alpha)$ , which is the reaction model that depends on the reaction mechanism. According to the above-mentioned equations, the plots of  $\ln \beta$  versus  $1000/T$  (Equation 6) and  $\ln(\beta/T^2)$  versus  $1000/T$  (Equation 7) corresponding to different extents of conversion  $\alpha$  can be obtained by a linear regression of the least squares method. The activation energies  $E$  and pre-exponential factor  $A$  can be evaluated from the slopes and intercepts of the straight lines with better linear correlation coefficients ( $r^2$ ), respectively. The activation energies were calculated at the heating rates of 5, 10, 15, 20, and 25  $^\circ\text{C min}^{-1}$  via these methods in the range of 0.1-0.9.

### III. EXPERIMENTAL DETAILS

#### A. Material

The crystalline form of IHT used in this study was supplied from Sigma Aldrich chemicals and it was confirmed by PXRD and DSC. The IHT is stored in refrigerator (2 to 8° C) in a closed container, to avoid any solid phase/form transformations due to the temperature and humidity.

#### B. Methods

##### I) TGA

Q5000IR Thermogravimetric Analyzer (TA instruments New Castle, DE) was used to study the dehydration kinetics of IHT. Approximately 10 mg of sample in an open aluminum pans were heated at four heating rates of 5, 10, 15, 20, and 25 °C min<sup>-1</sup> over the temperature range from 25 to 350 °C under dry nitrogen purge (60 mL/min) and the thermal transformation product was further characterized.

##### II) DSC

DSC was performed on a TA Instruments (New Castle, DE) Q1000 DSC with refrigerated cooling system. The temperature and cell constants were calibrated using Indium. The analysis was performed by taking 2 to 3 mg of sample encapsulated into aluminum sample pans with pierced aluminum lid and collected data at 10°C min<sup>-1</sup> over the temperature range from 30 to 350 °C in a N<sub>2</sub> atmosphere with the flow rate of 50 mL min<sup>-1</sup>.

##### III) PXRD

The experiments were carried out using PANalytical X'Pert PRO X-ray Powder Diffractometer using copper radiation K<sub>α1</sub> with X'Celerator detector. The instrument was calibrated using NIST standard reference material 1976a (Corundum) for relative intensities and 640C (Silicon) for Peak position. Each diffraction profile was collected using following setting parameters of the diffractometer: the X-Ray tube was operated at a voltage of 45 kV and current of 40 mA; Ni filtered Cu K<sub>α1</sub> radiation (λ = 1.5418 Å); scan type - continuous mode; scan range (2θ) 5° to 30°; step size 0.01° 2θ; time per step 20.8 sec. Data acquisition and analysis were performed on X'pert data collector and High Score Plus software's, respectively.

### IV. RESULTS AND DISCUSSIONS

#### C. Solid state characterization

The powder X-ray diffraction pattern of IHT was identical to that of IHT reported in the literature [6]. When heated in the TGA up to 350 °C (at 10 °C/min under nitrogen purge), a weight loss of 7.77%w/w (Fig. 2) was observed, which

Table 1. Thirteen Solid-State Rate and Integral Expressions for Different Reaction Models used for the present analysis

S.No.	Reaction Model	differential form $f(x) = 1/k dx/dt$	integral form $g(x) = kt$
<b>Nucleation models</b>			
1	Power Law	$x^{-3/4}$	$x^{1/4}$
2	Power Law	$x^{-2/3}$	$x^{1/3}$
3	Power Law	$x^{-1/2}$	$x^{1/2}$
4	Avrami-Erofeev	$4(1-x)^{-1} [-\ln(1-x)]^{3/4}$	$[-\ln(1-x)]^{1/4}$
5	Avrami-Erofeev	$3(1-x)^{-1} [-\ln(1-x)]^{2/3}$	$[-\ln(1-x)]^{1/3}$
6	Avrami-Erofeev	$2(1-x)^{-1} [-\ln(1-x)]^{1/2}$	$[-\ln(1-x)]^{1/2}$
<b>Diffusion models</b>			
7	One dimensional Diffusion	$x^{-1/2}$	$x^2$
8	Diffusion control (Janders)	$2(1-x)^{-2/3} [1-(1-x)^{1/3}]^{-1}$	$[1-(1-x)^{1/3}]^2$
9	Diffusion control (Crank)	$3/2[(1-x)^{-1/3}-1]^{-1}$	$1-2/3 - (1-x)^{2/3}$
<b>Reaction order and geometrical contraction models</b>			
10	Mampel (first order)	$1-x$	$[-\ln(1-x)]$
11	Second Order	$(1-x)^{-2}$	$(1-x)^{-1}-1$
12	Contracting cylinder	$2(1-x)^{-1/2}$	$1-(1-x)^{1/2}$
13	Contracting Sphere	$3(1-x)^{-2/3}$	$1-(1-x)^{1/3}$

Table 2. Activation Energy Values (E), Pre-exponential Factor (A), and Correlation Coefficient ( $r^2$ ) Calculated by Ozawa and KAS Methods for the Dehydration of IHT in an  $N_2$  Atmosphere

	Ozawa Method			KAS method		
	$E/kJ mol^{-1}$	$r^2$	$A/min^{-1}$	$E/kJ mol^{-1}$	$r^2$	$A/min^{-1}$
0.1	95.4	0.935	$7.97 \times 10^7$	95.2	0.954	$6.69 \times 10^7$
0.2	89.0	0.984	$5.26 \times 10^7$	88.3	0.982	$4.36 \times 10^7$
0.3	79.6	0.987	$4.64 \times 10^7$	78.3	0.985	$2.56 \times 10^7$
0.4	74.2	0.989	$3.52 \times 10^7$	72.5	0.988	$1.48 \times 10^7$
0.5	70.1	0.989	$2.02 \times 10^7$	68.1	0.987	$1.12 \times 10^7$
0.6	66.4	0.989	$1.00 \times 10^7$	64.2	0.987	$5.36 \times 10^6$
0.7	63.2	0.989	$4.02 \times 10^6$	60.7	0.987	$4.11 \times 10^6$
0.8	60.5	0.989	$2.27 \times 10^6$	57.8	0.987	$2.99 \times 10^6$
0.9	57.5	0.991	$1.09 \times 10^6$	54.6	0.988	$1.27 \times 10^6$
<b>Avg</b>	<b>72.9</b>	<b>0.982</b>	<b><math>3.53 \times 10^7</math></b>	<b>71.1</b>	<b>0.983</b>	<b><math>3.33 \times 10^7</math></b>

Table 3. Most Probable Mechanism Functions  $g(\alpha)$ , Slopes, and the Correlation Coefficients of Linear Regression ( $r^2$ ) at 60 °C and 65 °C during the Dehydration Process of IHT

Stage	Temperature (°C)	Mechanism No.	Slop	$r^2$
Dehydration	60	10	-0.974	0.997
		11	-1.297	0.994
		12	-0.837	0.997
		13	-0.981	0.997
	65	10	-1.144	0.994
		11	-1.819	0.975
		12	-0.89	0.997
		13	-0.968	0.997

agreed with the theoretical weight loss of 7.98%w/w for complete dehydration. TGA thermogram exhibits a single dehydration step over the range 25–110 °C in open-pan TGA. When IHT samples were subjected to DSC analysis under experimental conditions similar to those for TGA, the peak maximum temperature in the DSC curve agreed well with that for the dehydration step in TGA (Fig. 2) and the PXRD pattern obtained after dehydration shows distinguish with its initial pattern (Fig.3).

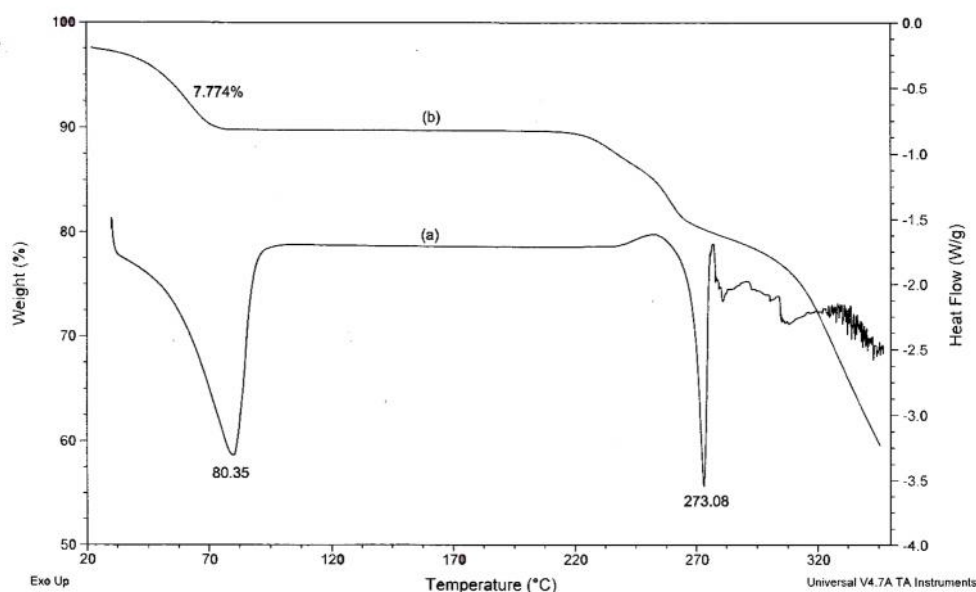


Figure 2. TGA and DSC curves of the IHT at a heating rate of  $10 \text{ }^\circ\text{C min}^{-1}$  in a  $N_2$  atmosphere

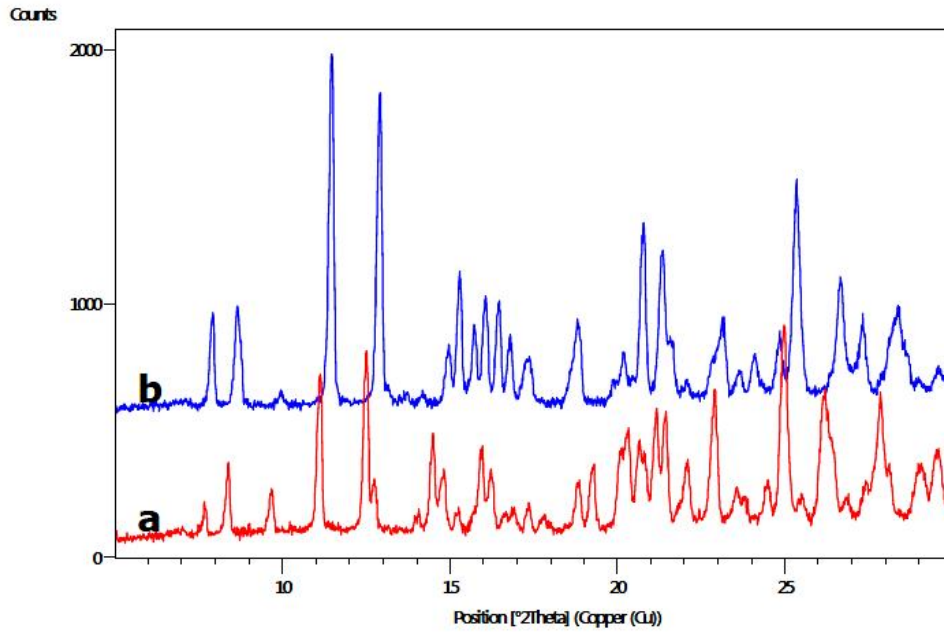


Figure 3. PXRD patterns of (a) the IHT and (b) the calcined IHT in a N<sub>2</sub> atmosphere

D. Kinetic Studies.

IV) Calculation of Activation Energy.

The Ozawa and KAS analysis results from four TGA measurements are presented in Figures 4 and 5, respectively. The activation energies  $E$  from these methods are listed in Table 2. According to Table 3, the activation energy values of dehydration step calculated from Ozawa and KAS methods were found to be 72.9 and 71.1 kJ mol<sup>-1</sup> respectively, which reveal that they agree well with each other. The difference of this value in both methods can be observed in a very small range (about 2 kJ mol<sup>-1</sup>). Hence, it can be concluded that the activation energy of non-isothermal decomposition of IHT is reliable.

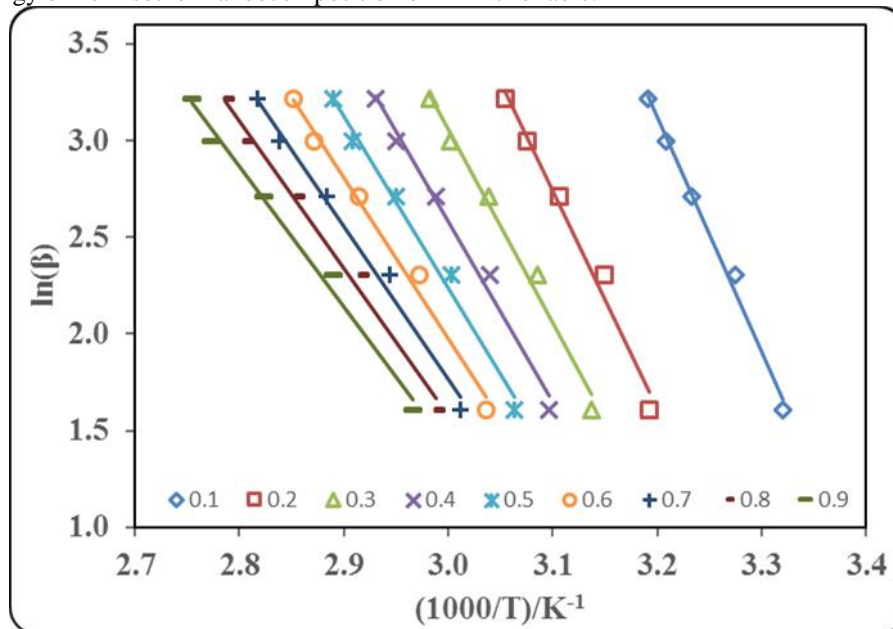


Figure 4. Ozawa plots for the dehydration process of IHT at four heating rates at various conversions ( $\alpha = 0.1-0.9$ , with 0.1 increment)

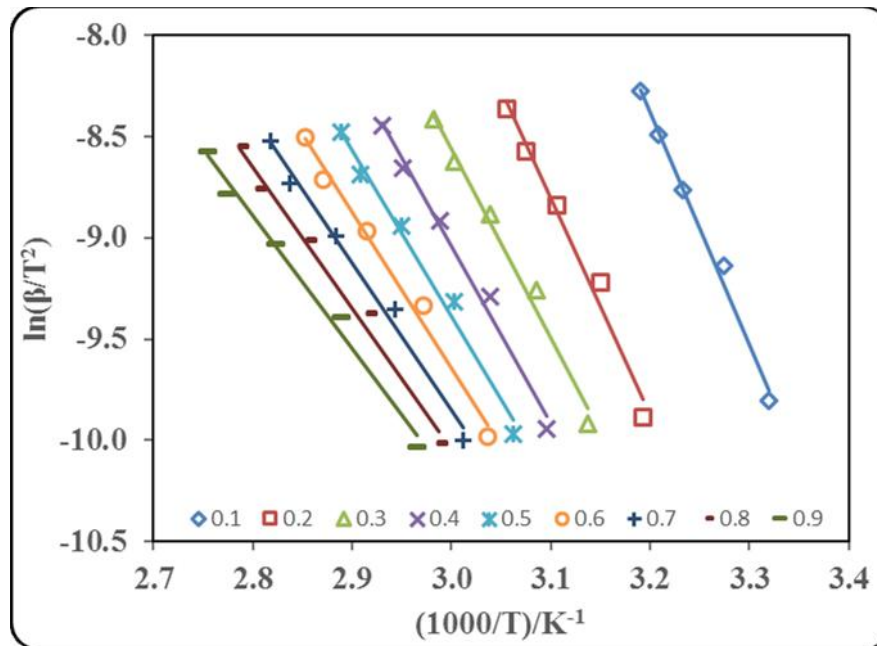


Figure 5. KAS plots for the dehydration process of IHT at four heating rates at various conversions ( $\alpha = 0.1-0.9$ , with 0.1 increment)

V) *Determination of the Most Probable Mechanism function and Pre-exponential Factor.*

The following equation will be used to estimate the most probable reaction mechanism:

$$\ln g(\alpha) = \left( \ln \frac{AE}{R} + \ln \frac{e^{-x}}{x^2} + \ln h(x) \right) - \ln S \quad (8)$$

Where,  $x$  is  $E/RT$  and  $h(x)$  is expressed by the fourth Senum and Yang approximation as described ref. [13]. To determine the most probable mechanism function, the degrees of conversion corresponding to four heating rates taken at the same temperature (we selected at 60 and 65 °C) were substituted into the left side of equation 9 for all 13 types of mechanism functions as presented in Table 1. If the mechanism function  $g(\alpha)$  according to Equation 9 exhibits the slope and the linear correlation coefficient  $r^2$  closest to -1.0000 and unity, respectively, then the function  $g(\alpha)$  is the most probable mechanism function. The results of the most probable mechanism functions during the dehydration process at 60 and 65 °C are tabulated in Table 3. According to Table 3, the slopes determined from the function nos. 10 and 13 are the closest to -1.000 and the correlation coefficients  $r^2$  were suited best. The mechanism function no. 13 was selected as the most probable mechanism function, because the slopes and correlation coefficients  $r^2$  were nearly constant at two temperatures. In addition, the slope from this function shows the best value. Therefore, it can be stated that the mechanism function with the integral form  $g(\alpha) = 1 - (1 - \alpha)^{1/3}$  and differential form  $f(\alpha) = 3(1 - \alpha)^{2/3}$  belongs to the mechanism of phase boundary reaction (spherical symmetry). This type of mechanism is assumed that the nucleation occurs rapidly on the surface of the crystal. The rate of dehydration is controlled by the resulting reaction from the interface progresses toward the center of the crystal [14]. The pre-exponential factor  $A$  can be estimated from the intercept of the plots from Ozawa (Equation 6) and KAS (Equation 7) equations by inserting the most probable function  $g(\alpha)$  and the activation energy into the intercepts of these plots. The obtained pre-exponential factors  $A$  from Ozawa and KAS calculations are tabulated in Table 3. It can be seen that the values of pre-exponential factor  $A$  regularly decrease with an increasing degree of conversion  $R$  for both the Ozawa and KAS models. These  $A$  values are the measure of the collision frequencies and were found to be  $3.53 \times 10^7$  and  $3.33 \times 10^7 \text{ min}^{-1}$ , respectively. The average pre-exponential factors from the Ozawa method agree well with the KAS method.

V. CONCLUSION

Our work on the dehydration kinetics of the IHT reveals the following characteristics.

- a) The mechanism of the dehydration process is the phase boundary reaction (spherical symmetry), by which the rate of this process is controlled by the resulting reaction interface progresses toward the center of the crystal.
- b) The kinetic study of thermal dehydration of this compound was carried out by using Ozawa and KAS methods, which reveal that the average calculated activation energy's and pre-exponential factors values are close to each other.

REFERENCE

- [1] A. Ravikiran,, M. Arthanareeswari, P. Kamaraj, C. Praveen and K. Pavan, "Dehydration Kinetics of Sibutramine Hydrochloride Monohydrate," Chem Sci Trans., 2(S1), pp. S288-S294, (2013)/ DOI:10.7598/cst2013.28.
- [2] Khawam, A. "Application of solid-state kinetics to desolvation reactions," Theses and Dissertations, University of Iowa , pp. 1-48, 2007.
- [3] A. Ravikiran, M. Arthanareeswari, P. Kamaraj, and C. Praveen, "Nonisothermal Kinetics Analysis of the dehydration of Ziprasidone Hydrochloride Monohydrate by Thermogravimetry," Indian J. Pharm. Sci., 75(3), pp.361-364, 2013.
- [4] S. Byrn, , Pfeiffer, R., Ganey, M., Hoiberg, C., & Poochikian, G, 'Pharmaceutical solids: a strategic approach to regulatory considerations,' Pharmaceutical Research, 12(7), 945-954,1995.
- [5] D. Zhou, E.A. Schmitt, G.G.Zhang, D. Law, C.A. Wight, S. Vyazovkin and D.J. Grant, "Model-free treatment of the dehydration kinetics of nedocromil sodium trihydrate," Journal of pharmaceutical sciences, 92(7), 1367-1376,2003.
- [6] Ganpat Dan Shimbhu Charan, Arun Ankush Tanpure, Kumar Kamlesh Laxmi Singh, "(S)-4,11-diethyl-3,14-dioxo-3,4,12,14-tetrahydro-1H-pyrano [3',4':6,7] indolizino [1.2-b]quinoline-4,9-diyl bis([1,4'-bipiperidine]-carboxylate and its use", Patent No. EP 2399919 A1.
- [7] C. Praveen, M. Arthanareeswari, A. Ravikiran,P. Kamaraj and K. Pavan, "Kinetic studies on crystallization process of amorphous Vilazodone hydrochloride" Int J Pharm Pharm Sci. vol.5,pp.636-638,2014.
- [8] H.E. Kissinger, "Reaction kinetics in differential thermal analysis," Analytical chemistry, 29(11), pp. 1702-1706, 1957.
- [9] T. Ozawa "A new method of analyzing thermogravimetric data," Bulletin of the chemical society of Japan, 38(11), pp. 1881-1886, 1965.
- [10] T. Akahira and T. Sunose: Trans. Joint Convention of Four Electrical Institutes, paper no. 246 (1969) Research Report, Chiba Institute of Technology, Sci. Technol. Vol.16, pp. 22-31, 1971.
- [11] A.W.Coats and J.P. Redfern, "Kinetic parameters from thermogravimetric data," Nature, vol. 201, pp. 68 - 69, 1964. doi:10.1038/201068a0.
- [12] D.W.Van Krevelens, and P.J. Hoftijzer, "Kinetics of gas-liquid reaction-general theory," Trans I Chem E, vol. 32, pp. 5360-83,1964.
- [13] G.I. Senum, R.T.Yang, "Rational approximations of the integral of the Arrhenius function," J. Therm. Anal. Calorim.vol.11,pp. 445,1977.
- [14] A. Khawam, D.R. Flanagan, "Solid-State Kinetic Models: Basics and Mathematical Fundamentals," J. Phys. Chem. B., vol. 110, pp. 17315, 2006.